Title: New Extraction of the Proton Radius from ep-Scattering Data

Date: Sep 08, 2015 01:00 PM

URL: http://pirsa.org/15090017

Abstract: <p>A new analysis of electron-proton scattering data (those published in 2010 by the Mainz A1 collaboration and previous world compilations) to determine the proton electric and magnetic radii is presented. The analysis enforces model-independent constraints of form factor analyticity and investigates a wide range of possible systematic effects. Employing standard models for radiative corrections, our improved analysis yields proton electric radii for the Mainz and world data sets that are consistent, although a simple combination yields a value r_E = 0.904(15) fm that is 4-sigma larger than the CREMA muonic hydrogen determination. Remaining possible deficiencies are discussed that, if addressed, could reconcile the values from muonic hydrogen spectroscopy and ep-scattering.</p>

Outline

r_E^P before 2010

0.8768	± 0.0069			MOHR	08	RVUE	2006 CODATA value
0.844	$^{+0.008}_{-0.004}$			BELUSHKIN	07		Dispersion analysis
0.897	± 0.018			BLUNDEN	05		SICK 03 + 2γ correction
0.8750	± 0.0068			MOHR	05	RVUE	2002 CODATA value
0.895	± 0.010	± 0.013		SICK	03		$ep \to ep$ reanalysis
0.830	± 0.040	± 0.040	24	ESCHRICH	01		$ep \to ep$
0.883	± 0.014			MELNIKOV	00		1S Lamb Shift in H
0.880	± 0.015			ROSENFELDR.	00		ep + Coul. corrections
0.847	± 0.008			MERGELL	96		ep + disp. relations
0.877	± 0.024			WONG	94		reanalysis of Mainz ep data
0.865	± 0.020			MCCORD	91		$ep \to ep$
0.862	± 0.012			SIMON	80		$ep \to ep$
0.880	± 0.030			BORKOWSKI	74		$ep \to ep$
0.810	± 0.020			AKIMOV	72		$ep \to ep$
0.800	± 0.025			FREREJACQ...	66		$ep \to ep$ (CH_2 tgt.)
0.805	± 0.011			HAND	63		$ep \to ep$

PDG, 2012

Two developments in 2010:

- High-statistics, precision ep-scattering experiment at MAMI by the A1 collaboration.
- New spectroscopic measurements in μp at PSI.

r_E and the Hydrogen Energy Spectrum

Recall

$$-E_n \sim \frac{R_\infty}{n^2} + \frac{2}{3}\frac{(Z\alpha)^4}{n^3} m_r^3 r_E^2 \delta_{l0} \,,$$

$$R_\infty = \frac{m_r \alpha^2}{2} \,.$$

The well-measured $1S - 2S$ transition is dependent on both R_∞ and r_E.
We can separate the "finite-size" contribution by:

- Another atomic H transition (e.g. $2S - 8S$),
- ep-scattering experiments,
- μp transition ($2S - 2P$).

In μp, $m_r^3 \sim 10^7 m_e^3$, and the effect of r_E is enhanced by the smaller Bohr radius.

r_E and the Hydrogen Energy Spectrum

Recall

$$-E_n \sim \frac{R_\infty}{n^2} + \frac{2}{3}\frac{(Z\alpha)^4}{n^3} m_r^3 r_E^2 \delta_{l0}\,,$$
$$R_\infty = \frac{m_r \alpha^2}{2}\,.$$

The well-measured $1S - 2S$ transition is dependent on both R_∞ and r_E.
We can separate the "finite-size" contribution by:

- Another atomic H transition (e.g. $2S - 8S$),
- ep-scattering experiments,
- μp transition ($2S - 2P$).

In μp, $m_r^3 \sim 10^7 m_e^3$, and the effect of r_E is enhanced by the smaller Bohr radius.

Measurement of Lamb Shift with Muonic Hydrogen

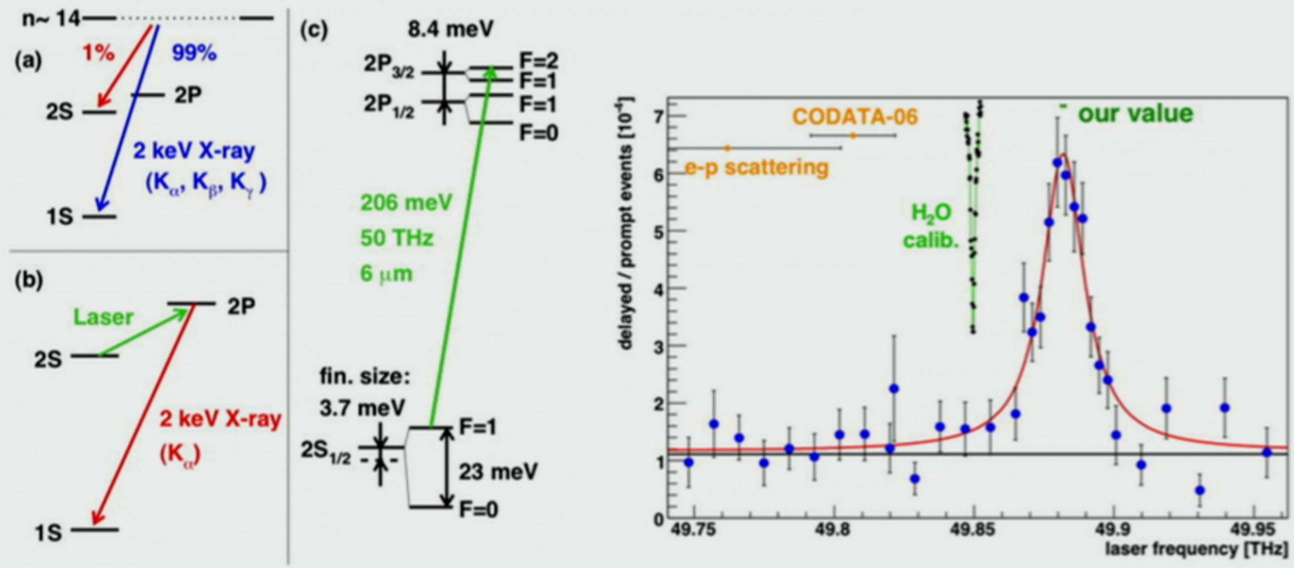

- The metastable 2S state is excited to the 2P state using a laser about $t_{2S} = 1\ \mu$s after the formation of the muonic hydrogen atoms. Pohl et al. (2010), Antognini et al. (2013)
- If it is on resonance, delayed 2 keV photons are detected in coincidence with the laser.
- The vacuum polarization is dominant in determining the level splitting, but the proton radius has an effect with $\Delta E \propto m_r^3$ (reduced mass), and $m_\mu / m_e \sim 200$. Effect is $\sim 2\%$ for μp: $\Delta E^{\text{theory}}_{2S-2P} \sim 209.98 - 5.23 r_E^2 + 0.03 r_E^3$ meV, r_E in fm.

r_E and ep Scattering

- Mott cross-section for scattering of a relativistic electron off a recoiling point-like proton is

$$\left(\frac{d\sigma}{d\Omega}\right)_M = \frac{\alpha^2}{4E^2 \sin^4\frac{\theta}{2}} \cos^2\frac{\theta}{2} \frac{E'}{E}.$$

- The Rosenbluth formula generalizes the above,

$$\left(\frac{d\sigma}{d\Omega}\right)_R = \left(\frac{d\sigma}{d\Omega}\right)_M \frac{1}{1+\tau}\left[G_E^2 + \frac{\tau}{\epsilon} G_M^2\right],\ \tau = \frac{-q^2}{4M^2},\ \epsilon = \frac{1}{1+2(1+\tau)\tan^2\frac{\theta}{2}}.$$

- The Sachs form factors $G_E(q^2), G_M(q^2)$ account for the finite size of the proton. In terms of the standard Dirac (F_1) and Pauli (F_2) form factors,

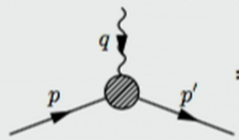

$$= \Gamma^\mu(q^2) = \underbrace{\frac{G_E + \tau G_M}{1+\tau}}_{F_1(q^2)} \gamma^\mu + \frac{i}{2M}\sigma^{\mu\nu} q_\nu \underbrace{\frac{G_M - G_E}{1+\tau}}_{F_2(q^2)}.$$

- The radii are defined by

$$\langle r^2 \rangle \equiv \frac{6}{G(0)} \frac{\partial G}{\partial q^2}\Big|_{q^2=0},\quad G_E^p(0) = 1, G_M^p(0) = \mu_p.$$

r_E^P since 2010

r_p = 0.84184(67) fm *Pohl, R. et al., Nature 466, 213-217 (2010)*
r_p = 0.84087(39) fm *Antognini. et al., Science 339, 417 (2013)*

Unprecedented precision

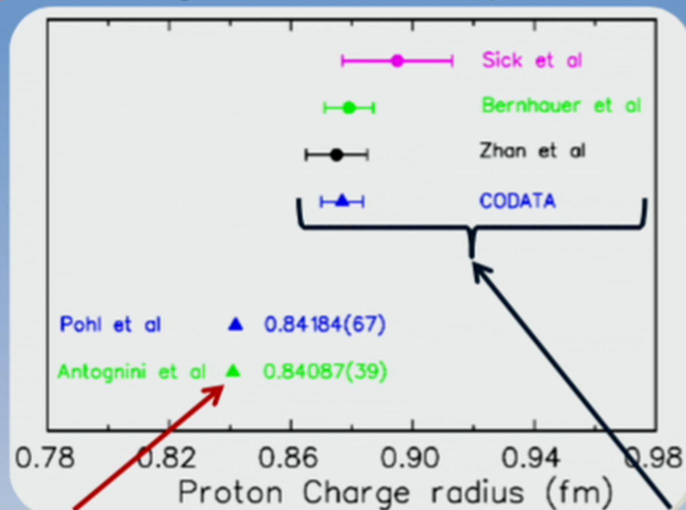

- **7σ discrepancy between muonic and average electronic measurements !**
- **Results from electronic and scattering measurements agree**

From M. Meziane

We perform a reanalysis of the ep-scattering data and simultaneously fit the charge and magnetic radii of the proton.

Further Motivation

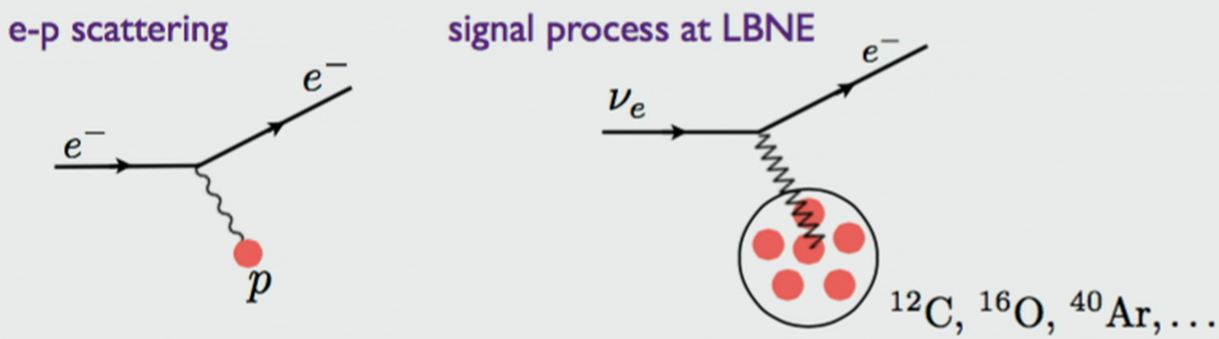

From R. Hill

The assumptions and tools used in the ep scattering analysis also appear in the νN scattering literature.
An investigation of these in the simpler ep scenario is crucial to the future νN scattering precision program.

Dataset Nomenclature

We consider data with maximum momentum transfer $Q^2 < 1.0$ GeV^2. We split the available elastic ep-scattering data into two datasets:

- **"Mainz"**: high-statistics dataset, 1422 data points in the full dataset with $Q^2_{\text{max}} < 1.0$ GeV^2. Bernauer et al. (2014)
- **"world"**: compilation of datasets from other experiments, 363 data points plus 43 polarization measurements for $Q^2_{\text{max}} < 1.0$ GeV^2. see e.g. Arrington et al. (2003, 2007), Zhan et al. (2011)

Polarization experiments directly measure the form factor ratio $(\mu_p G_E)/G_M$.

Aside: χ^2 fitting uses the optimize.leastsq in SciPy.

Outline

Earlier Ansäntze for G_E, G_M

$$\left(\frac{d\sigma}{d\Omega}\right)_R = \left(\frac{d\sigma}{d\Omega}\right)_M \frac{1}{1+\tau}\left[G_E^2 + \frac{\tau}{\epsilon}G_M^2\right]$$

Earlier analyses used simple functional forms for G_E, G_M:

$$G_{\text{poly}}(q^2) = \sum_{k=0}^{\infty} a_k (q^2)^k \,, \qquad \text{polynomials/Taylor expansions,}$$

$$G_{\text{invpoly}}(q^2) = \frac{1}{\sum_{k=0}^{\infty} a_k (q^2)^k} \,, \qquad \text{inverse polynomials,}$$

$$G_{\text{cf}}(q^2) = \frac{1}{a_0 + a_1 \frac{q^2}{1+a_2 \frac{q^2}{1+\dots}}} \,, \qquad \text{continued fractions.}$$

In practice, we truncate the number of coefficients in the expansion at some k_{max}.
The above functional forms exhibit pathological behaviour with increasing k_{max}. Hill & Paz (2010)

The Bounded z Expansion

- QCD constrains the form factors to be analytic in $t = q^2$ outside of a time-like cut beginning at $t_{\text{cut}} = 4m_\pi^2$, the two-pion production threshold. Clearly this presents an issue with convergence for expansions in the variable q^2. Hill & Paz (2010)

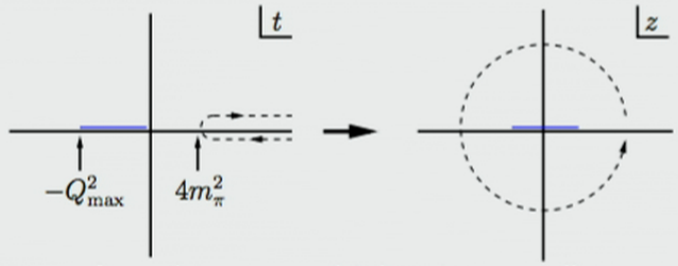

$$z(t; t_{\text{cut}}, t_0) = \frac{\sqrt{t_{\text{cut}} - t} - \sqrt{t_{\text{cut}} - t_0}}{\sqrt{t_{\text{cut}} - t} + \sqrt{t_{\text{cut}} - t_0}}$$

- By a conformal map, we obtain a true small-expansion variable z for the physical region.

$$G_E = \sum_{k=0}^{k_{\text{max}}} a_k [z(q^2)]^k\,, \quad G_M = \sum_{k=0}^{k_{\text{max}}} b_k [z(q^2)]^k\,.$$

- Q^2_{max} is the maximum momentum transfer in a given set of data.
- t_0 is the point that is mapped to $z(t_0) = 0$. We have used the simple choice $t_0 = 0$, but have checked that the results do not vary significantly for the choice t_0.
- By including other data, such as from $\pi\pi \to N\bar{N}$ or $e^+e^- \to N\bar{N}$ production, it is possible to move the t_{cut} to larger values, improving the convergence of the expansion.

Sensitivity of Statistical Uncertainties to Q^2_{max}

Scattering data at low Q^2 determines r_E, since it is defined as the slope of G_E at $q^2 = 0$.

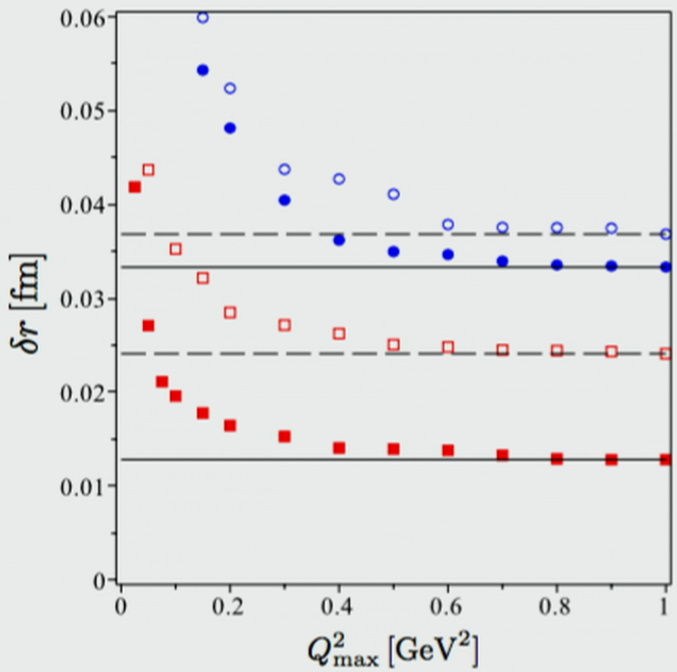

- Filled: Mainz, hollow: world+pol
- r_E
- r_M

Bounded z expansion, statistics-only errors.

Bounded z Expansion Fit to Mainz Data

Using $t_0 = 0$, $k_{\text{max}} = 12$, $|a_k|_{\text{max}} = 5$, $|b_k|_{\text{max}} = 5\mu_p$, with a Gaussian bound on a_k, b_k in χ^2.

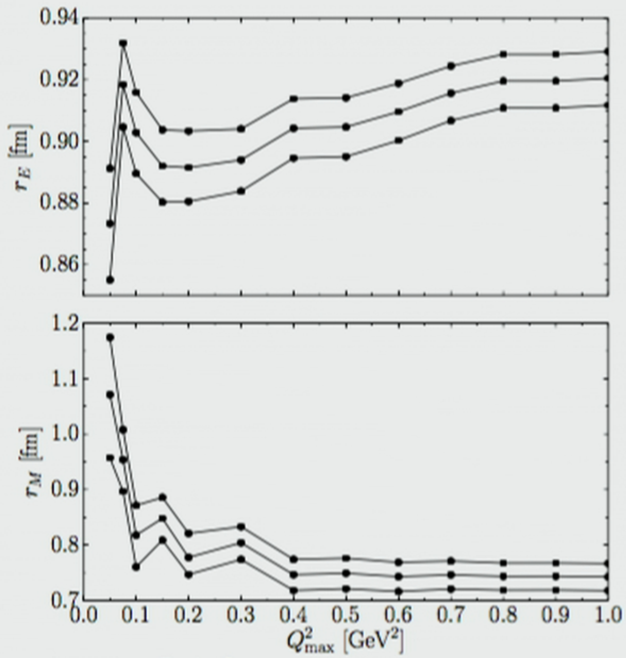

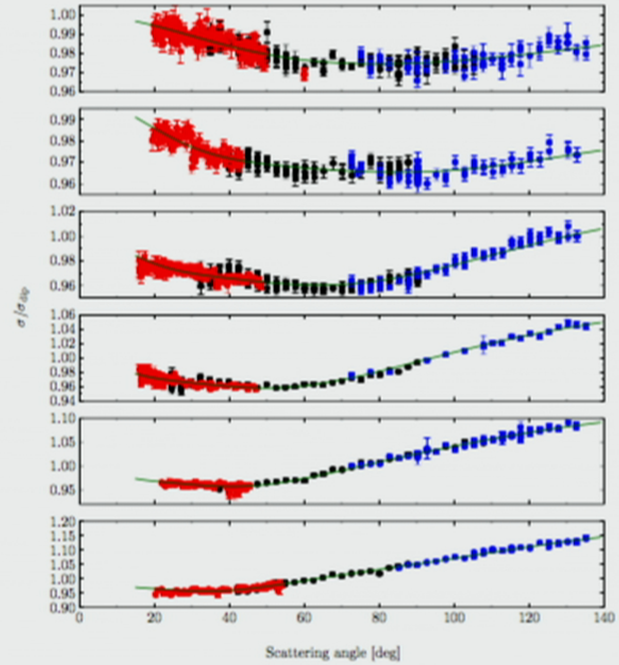

spectrometer: B, A, C

For $Q^2_{\text{max}} = 1.0$ GeV^2, $r_E = 0.920(9)$ fm, $r_M = 0.743(25)$ fm (statistics-only errors).

k_{max} Dependence

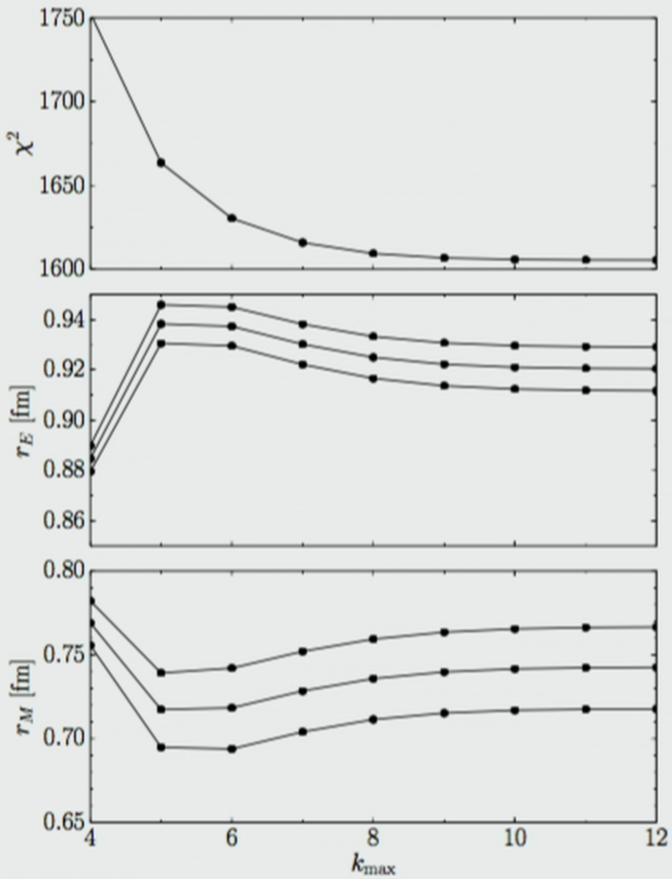

- We can also test the dependence of the fit results on the choice of k_{max}.
- The fit has converged for $k_{\text{max}} = 10$.
- We use a default of $k_{\text{max}} = 12$ in fits.

Unbounded Fits

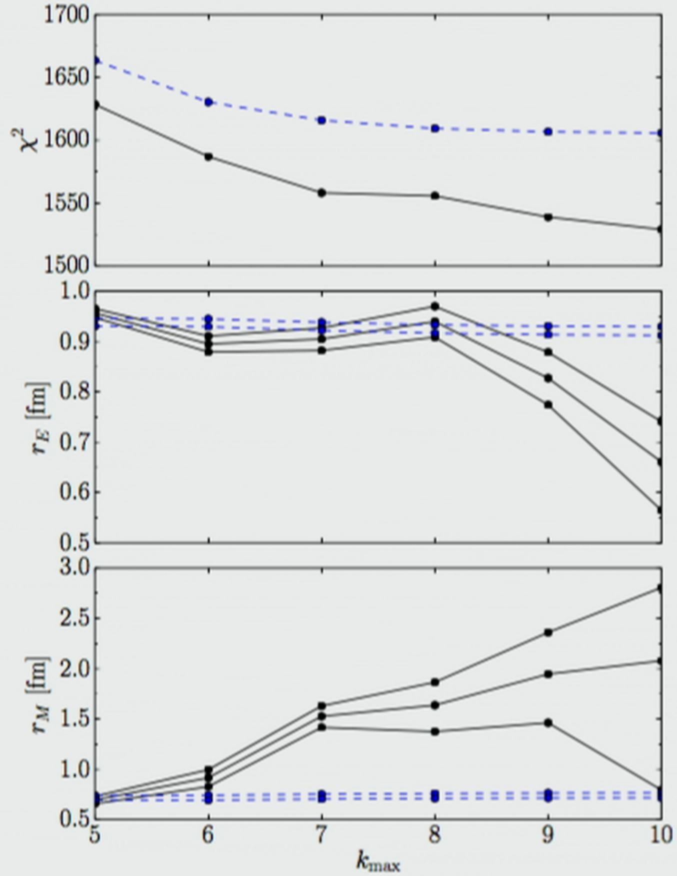

- The Sachs form factors are known to fall off as Q^4 up to logs for large Q^2, so coefficient values cannot be arbitrarily large.
- To test enlarging the bound, we took $|a_k|_{\text{max}} = |b_k|_{\text{max}}/\mu_p = 10$, and found $r_E = 0.916(11)$ fm, $r_M = 0.752(34)$ fm.
- However, as $|a_k|_{\text{max}} \to \infty$, $|a_k|$ for large k takes on unreasonably large values, in conflict with QCD.

Outline

One-Loop $\mathcal{O}(\alpha)$ Radiative Corrections

- The proton form factors are defined in the one-photon exchange approximation. A consistent definition of the form factors is required to compare extracted radii.

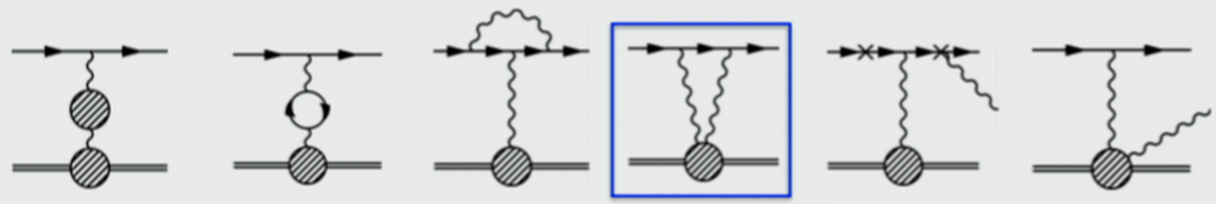

- We know how to compute results for the electron vertex correction and the leptonic contributions to the vacuum polarization in perturbation theory.
- From previous dispersive analyses of $e^+e^- \to$ hadrons data, we expect the correction from hadronic vacuum polarization to be smaller than current achieved precision in scattering experiments. Jegerlehner (1996), Friar et al. (1999)
- For soft bremsstrahlung and two-photon exchange (TPE), there are two conventions for subtraction of infrared divergences. Tsai (1961), Maximon & Tjon (2000)
- At present, we cannot calculate the remainder of the TPE contribution from first principles.

Finite TPE Corrections

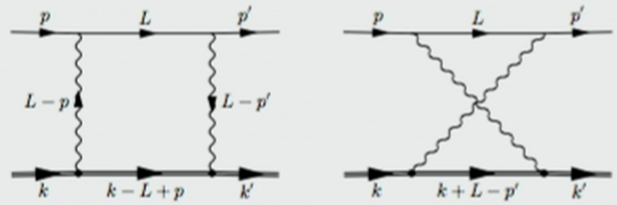

- The standard procedure for modelling the finite part of the TPE is by "Sticking in Form Factors" (SIFF). Treat the proton as a propagating Dirac particle and insert Γ^μ at each of the vertices, using simple form factor ansätze for F_1, F_2. Blunden et al. (2003, 2005)
- We investigated the model dependence of this calculation:

$$F_1 = F_2/(\mu_p - 1) = (1 - q^2/\Lambda^2)^{-1}\,, \qquad \text{monopole, } \Lambda^2 = 0.71\text{ GeV}^2\,,$$

$$F_1 = F_2/(\mu_p - 1) = (1 - q^2/\Lambda^2)^{-2}\,, \qquad \text{dipole, } \Lambda^2 = 0.71\text{ GeV}^2\,,$$

$$F_i = \sum_{j=1}^{3} \frac{a_{ij}}{b_{ij} - q^2}\,, \quad \sum_{j=1}^{3} \frac{a_{ij}}{b_{ij}} = F_i(0)\,, \qquad \text{Blunden et al. sum of monopoles (2005).}$$

- The A1 collaboration instead applies the Feshbach correction McKinley & Feshbach (1948)

$$\delta_F = \alpha\pi \frac{\sin(\theta/2)(1 - \sin(\theta/2))}{\cos^2(\theta/2)} > 0\,,\,,$$

which is the $Q^2 = 0$ limit of the Coulomb distortion computed by Rosenfelder. It can also be understood as the scattering of soft photons in the $M_p \to \infty$ limit. Rosenfelder (1999)

Effect of TPE on Fit to Mainz Dataset

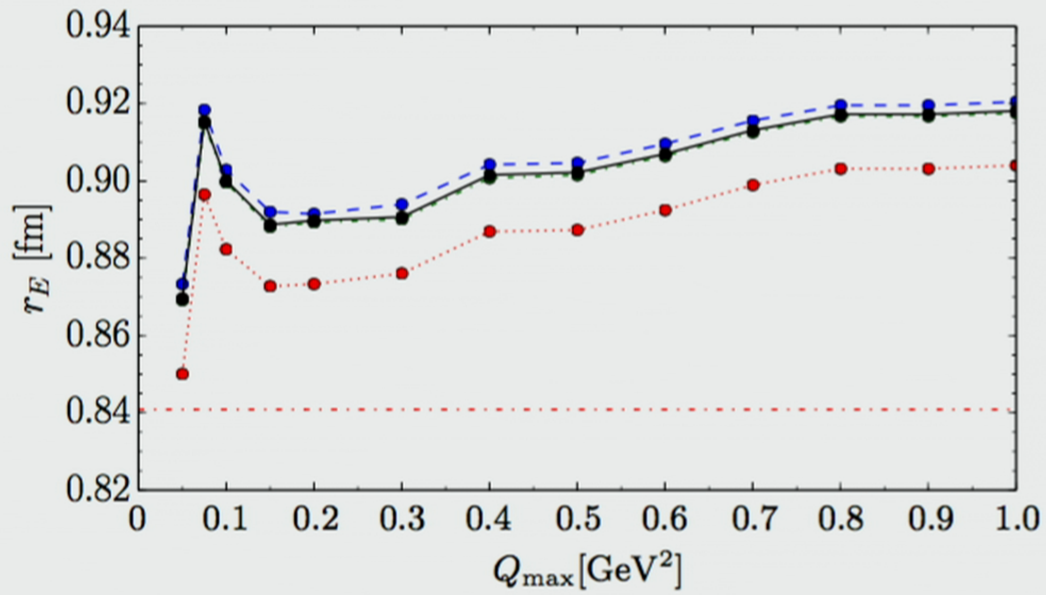

- No finite TPE correction.
- Feshbach: used by default in A1 collaboration's analysis of Mainz dataset.
- SIFF dipole
- SIFF Blunden: used in previous analyses of world dataset.

We use the Blunden convention for the remainder of the fits.

Behaviour of Different TPE Correction Models

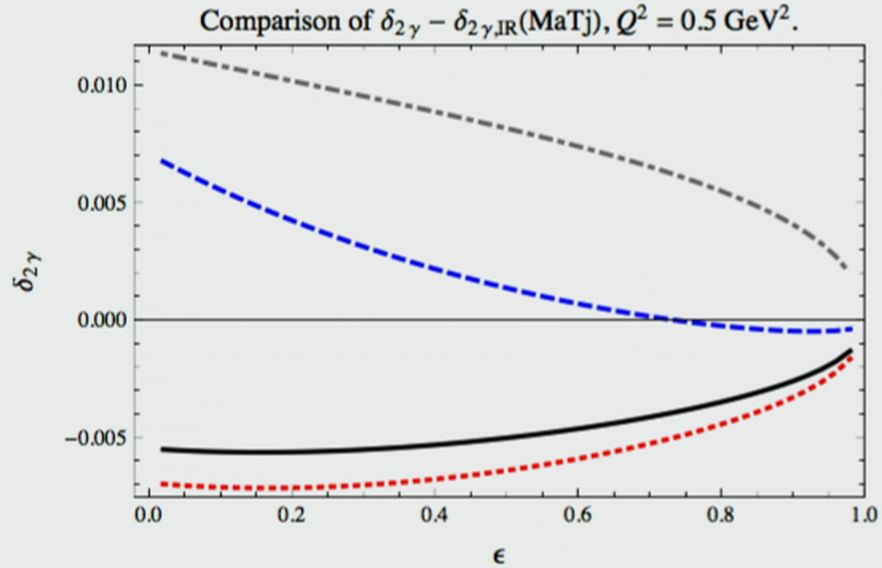

Feshbach, monopole, Blunden, dipole
$\epsilon \to 0$ is backscattering, $\epsilon \to 1$ is forward scattering.

For larger Q^2 values (above 0.5 GeV^2), the Blunden finite TPE correction does not grow with increasing Q^2, but changes sign. This is the behaviour required to resolve the discrepancy in world (Rosenbluth) and polarization measurements of the ratio $(\mu_p G_E)/G_M$. Blunden et al. (2005)

Outline

The A1 Approach

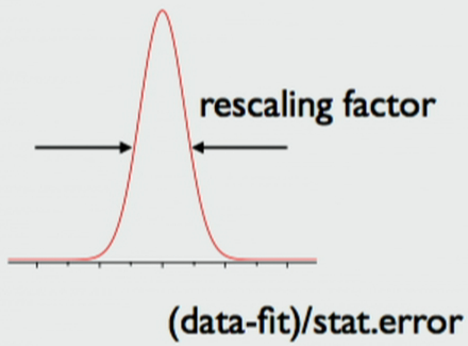

- The A1 analysis groups the Mainz dataset into 18 subsets: 3 spectrometers × 6 beam energies.
- For each subset, the differences between the fit and measured cross sections, scaled by the uncertainties, are fit to a Gaussian.
- The width of the Gaussian is used as the scaling factor κ for the statistical uncertainties in the subset.

Concerns:

- In the A1 analysis, the χ^2_{red} for the fit to the entire dataset with scaled errors is ≈ 1.15.
- In our bounded z expansion fit, we find χ^2_{red} per subset similar to the A1 Gaussian widths.
- Expressing the total A1 uncertainties as quadrature sums of statistical and uncorrelated uncertainties,

$$d\sigma_{i,\text{A1}} = \kappa_i d\sigma_{i,\text{stat}} = \sqrt{d\sigma^2_{i,\text{stat}} + d\sigma^2_{i,\text{syst}}},$$

  $d\sigma_{\text{syst}}$ is as low as 0.05% for some points.
- Multiple data points at the same kinematic settings drive the "effective systematic uncertainties" even lower.
- Random or time-dependent variations are experimentally difficult to constrain below 0.1%.

Rebinning

Some systematic uncertainties are not explicitly accounted for by the A1 analysis:

- time-dependent efficiencies,
- rate-dependent variations,
- beam-energy uncertainties,
- spectrometer angle offsets.

We would expect these uncertainties to be identical for the repeated measurements. Simply adding a fixed systematic to all points in the dataset would underestimate the systematic error for these repeated data points. We therefore combine these before adding a fixed systematic to the statistical uncertainty in quadrature.
We perform the following:

- Remove one set of points at $E_{\text{beam}} = 315$ MeV, $\theta = 30.01^\circ$ with inconsistent scatter.
- Identify 407 kinematic settings with multiple data points.
- "Rebin" these to obtain a dataset of 657 points.

Constant Systematics

After rebinning, we investigate the effect of adding a 0.25% and a 0.3% fixed systematic, e.g. for a data point with cross section σ_i,

$$d\sigma_i = \sqrt{d\sigma^2_{i,\text{stat}} + (0.003\sigma_i)^2}\,.$$

spec.	beam	N_σ	χ^2_{red}	CL (%)	χ^2_{red}	CL (%)
A	180	29	0.59	96.1	0.46	99.4
	315	23	0.54	96.4	0.44	99.1
	450	25	1.52	4.8	1.00	46.7
	585	28	1.54	3.4	1.03	42.8
	720	29	1.05	39.9	0.87	66.4
	855	21	0.92	56.8	0.77	76.0
B	180	61	0.85	79.8	0.65	98.3
	315	46	1.05	38.5	0.76	88.5
	450	68	0.90	71.7	0.67	98.2
	585	60	0.61	99.2	0.50	99.96
	720	57	1.29	6.9	0.97	53.7
	855	66	1.88	0.002	1.15	19.6
C	180	24	0.88	63.3	0.68	88.0
	315	24	1.16	27.2	0.78	76.8
	450	25	1.53	4.3	1.08	35.9
	585	18	0.83	66.3	0.65	86.4
	720	32	1.11	30.2	0.90	62.3
	855	21	0.79	73.7	0.62	90.5

Cols. 4 and 5 (6 and 7) give the results after the inclusion of a uniform 0.25% (final 0.3–0.4%) uncorrelated systematic. The 0.4% applies to $E_{\text{beam}} = 855$ MeV, spec B.

Fitting the rebinned dataset after these two modifications, we find $r_E = 0.908(13)$ fm & $r_M = 0.766(33)$ fm.

Outline

The A1 Approach (Again)

In the Mainz dataset, each data point includes three additional quantities:

- two cross sections corresponding to variations on the bremsstrahlung energy cut,
- kinematic-dependent factor, linear in the scattering angle θ, which accounts for efficiency changes, normalization drifts, variations in spectrometer acceptance, and background misestimations.

The entire dataset is refit either:

- using the minimum or maximum cross sections from variations on the energy cut,
- dividing or multiplying central values of the cross sections by the linear factor.

In each case, the largest difference of the resulting fit from the central values is taken as the difference, and

$$\Delta r_{\text{syst}} = \sqrt{(\Delta r_{\text{Ecut}})^2 + (\Delta r_{\text{corr}})^2}\,.$$

We find the energy cut has little impact on the radius central values: translates to an uncertainty in r_E of 0.003 fm and in r_M of 0.009 fm.

Our Approach

The linear factor is written as

$$1 + \delta_{\text{corr}} = 1 + a\frac{x - x_{\text{min}}}{x_{\text{max}} - x_{\text{min}}} .$$

In the A1 analysis:

- $x = \theta$,
- 18 values of $\theta_{\text{max}}, \theta_{\text{min}}$ for each spectrometer-E_{beam} subset,
- $a \approx$ 0.2%, same sign for all subsets.

We choose:

- $x = \theta, 1/\theta, Q^2, 1/Q^2, E', 1/E', 1/\sin^4(\theta/2)$,
- Three groupings: by spec (3), spec-E_{beam} (18), and normalization (34),
- $a = 0.5\%$, and same sign.

Different variables modify the functional form of the correction within each subset; however, the endpoints are always fixed to have a correction of 0 and 0.5%.

Our Findings

x	$Q^2_{\max}$ [GeV^2]	Δr_E [fm]	Δr_M [fm]
Q^2	0.05	∓ 0.017	± 0.021
	0.5	∓ 0.016	∓ 0.022
	1	∓ 0.015	∓ 0.026
$1/Q^2$	0.05	± 0.041	∓ 0.046
	0.5	± 0.025	± 0.016
	1	± 0.023	± 0.021
θ	0.05	∓ 0.022	± 0.027
	0.5	∓ 0.018	∓ 0.021
	1	∓ 0.017	∓ 0.025
$1/\theta$	0.05	± 0.036	∓ 0.039
	0.5	± 0.024	± 0.018
	1	± 0.021	± 0.022

Multiplication (top sign) or division (bottom sign), spectrometer-E_{beam} (18)

- A factor of 2.5 bigger than the A1 analysis, mainly due to increase in a.
- Different variable choices yield similar results, largest effect from $1/Q^2$.

Our Findings (cont.)

- Norm. grouping (34) yielded uncertainties that were typically 20–30% larger for r_E compared to the spec-E_{beam} (18), with smaller increases for the uncertainty on r_M.
- Spec-only grouping yielded somewhat smaller uncertainties for r_E compared to the spec-E_{beam}, with larger increases for the uncertainty on r_M.
- Systematic effects could differ for the different spectrometers, and the combined effect might be enhanced or suppressed by the assumption of identical corrections (always multiplying or dividing, same sign).
- For r_M, we found some cases with cancellations between spectrometers when the linear correction was applied to all three spectrometers vs. applied to each spectrometer individually.

For final results, take uncertainties using $x = \theta$ as representative correlated systematic, and use $a \approx 0.4\%$, dividing the above corrections by $4/5$.
At $Q^2_{\text{max}} = 1$ GeV^2, this choice yields correlated systematic uncertainties of 0.014 fm and 0.020 fm for r_E and r_M.

Summary of r_E Thus Far

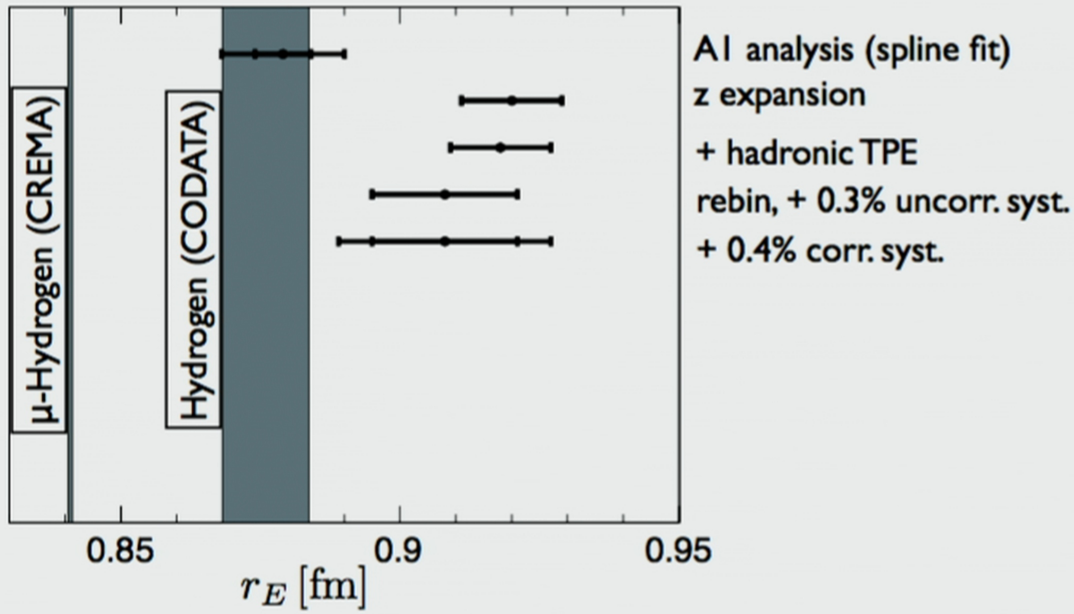

from R. Hill

$r_E = 0.908(13)(3)(14)$ fm & $r_M = 0.766(33)(9)(20)$ fm

We have expanded the A1 analysis of the correlated systematics, but have not made any drastic changes to the framework. A larger systematic shift to reconcile the values would require:

- a range of corrections larger than 0.4%,
- an extreme functional form,
- a "tuned" cancellation between subsets to reduce the overall systematic.

Fitting the a Parameters

- As an independent check, we can perform a fit assuming all the corrections are totally uncorrelated by performing a fit floating the parameters a_l for each subset l.
- We tested this using a Gaussian error of 0.4% for the a_l with the normalization grouping, finding:

Q^2_{max} [GeV^2]	r_{E,a_l} [fm]	r_{M,a_l} [fm]	r_E [fm]	r_M [fm]
0.5	$0.891(18)$	$0.792(49)$	$0.895(20)$	$0.776(38)$
1.0	$0.898(17)$	$0.781(48)$	$0.908(19)$	$0.766(40)$

- The uncertainties in this fit are somewhat smaller for the charge radius and larger for the magnetic radius, in line with the expectation based on applying the corrections separately to each spectrometer.
- While this may be an equally unrealistic assumption, a combined fit of the Mainz and world datasets would likely require this procedure.

r v Q^2_{max} for Final Fits

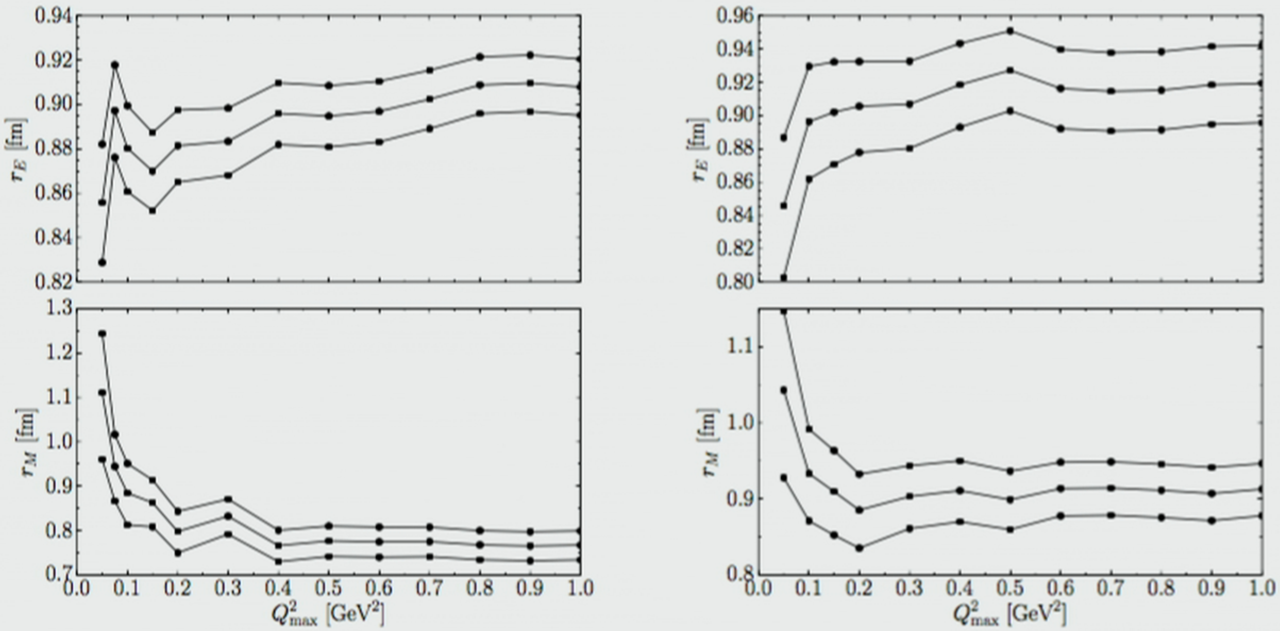

L: final fit to Mainz rebin dataset with 0.3/0.4% fixed systematic
R: final fit to world (incl. pol) dataset

$t_0 = 0, k_{\text{max}} = 12, |a_k|_{\text{max}} = |b_k|_{\text{max}}/\mu_p = 5$

Sensitivity, Revisited

Scattering data at low Q^2 determine radius, from its definition as the slope of the FF at $q^2 = 0$.

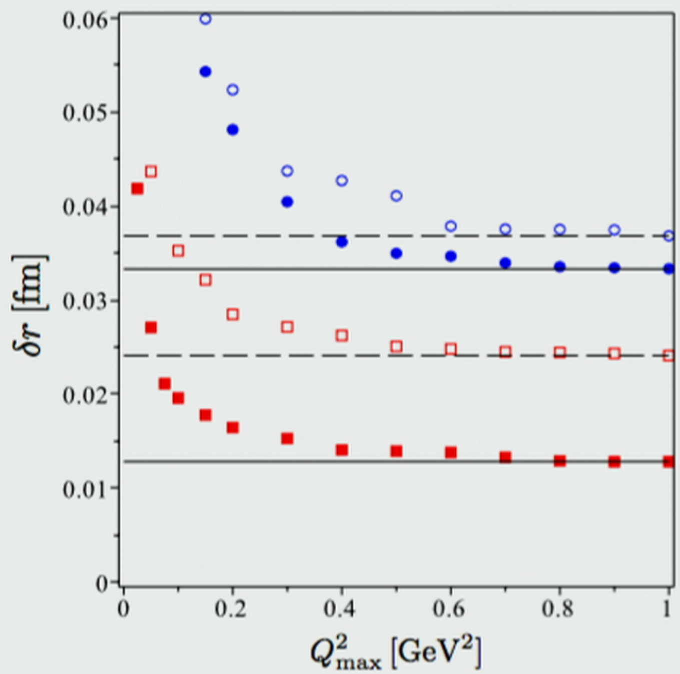

- Filled: Mainz, hollow: world+pol
- r_E
- r_M

Want to maximize sensitivity, but minimize effect of possible high Q^2 systematics.

Final Results for r_E

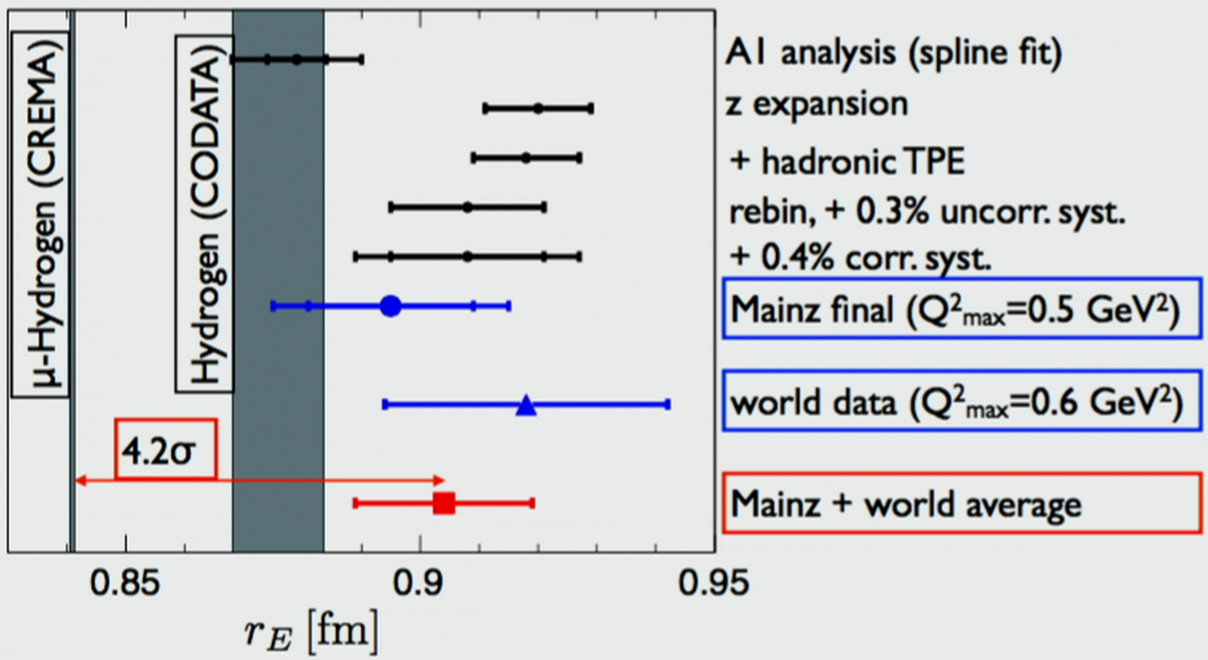

from R. Hill

$r_E^{\text{Mainz}} = 0.895(14)(14)$ fm, $r_E^{\text{world}} = 0.916(24)$ fm
$r_E^{\text{avg}} = 0.904(15)$ fm

A Possible Resolution: Large Logs

We have included scattering data with momentum transfers as large as $Q^2 \sim 1\,\mathrm{GeV}^2$.

- In this regime, QED perturbation theory breaks down due to large logarithms from electron radiative corrections

$$\frac{\alpha}{\pi}\log^2\frac{Q^2}{m_e^2}\bigg|_{Q^2\sim 1\,\mathrm{GeV}^2} \approx 0.5\,.$$

- Recall the sum of the first-order vacuum polarization and electron vertex and real bremsstrahlung corrections:

$$\delta = \frac{\alpha}{\pi}\left\{\left[\log\frac{Q^2}{m_e^2} - 1\right]\log\frac{(\eta\Delta E)^2}{EE'} + \frac{13}{6}\log\frac{Q^2}{m_e^2} + \dots\right\}.$$

  where ΔE is the detector energy resolution.

- When $Q \sim E \sim E'$ and $m_e \sim \Delta E$, the leading series of logarithms $\alpha^n \log^{2n}(Q^2/m_e^2)$ are resummed by making the replacement, Yennie, Frautschi, Yuura (1961)

$$1 + \delta \to \exp(\delta)\,.$$

One Scale?

- In practice, $\Delta E \gg m_e$, which can introduce another scale into the problem.
- As a check, we can instead multiply the cross sections by

$$(1+\delta) \to \left[1 \pm \left(\delta + \frac{\alpha}{\pi}\log^2\frac{Q^2}{m_e^2}\right)\right]^{\pm 1} \times \exp\left(-\frac{\alpha}{\pi}\log^2\frac{Q^2}{m_e^2}\right) ,$$

- This has the same 1-loop corrections, but resums the leading-logs when there is only one large ratio of scales, Q^2/m_e^2.

Large Logs (cont.)

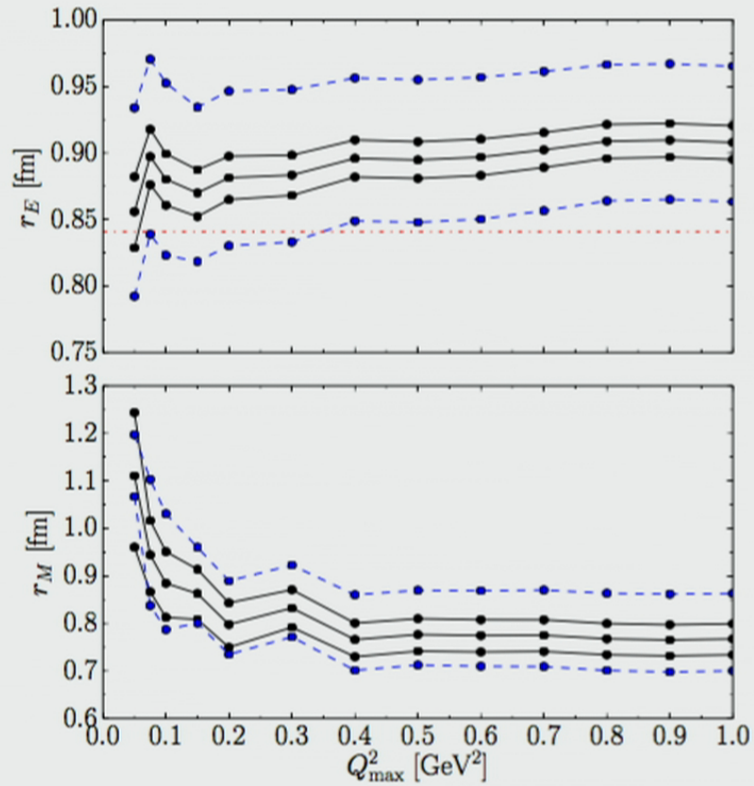

Black: fit to rebinned Mainz data with 0.3/0.4% fixed systematics, statistical uncertainties shown only.
$\Delta E = 10$ MeV, upper/lower blue curve are multiply/divide the $(1+\delta)$ factor.

Conclusion

- We presented the most comprehensive analysis of existing ep-scattering data:
  - using form factors constrainted by QCD,
  - performing careful studies of existing radiative correction models,
  - examining the uncorrelated systematics and rebinning the Mainz high-statistics dataset,
  - reconsidering systematic uncertainties.
- The Mainz and world values for r_E are consistent, but the simple combination of the Mainz and world values remains 4σ away from the μp spectroscopic value.
- We find a 2.7σ difference in the Mainz and world values for r_M.
- A possible resolution to the discrepancy involves modifying the large-log resummation of one-loop radiative corrections by considering intermediate energy scales neglected in standard analyses.
- Stay tuned for future experiments.
  - Low-Q^2 ($10^{-4} - 10^{-2}$ GeV^2) ep scattering. — PRad at JLAB, A1
  - μp scattering at PSI. — MUSE
  - Further measurements of H spectroscopy. — Vutha et al. (2012), Beyer et al. (2013), Peters et al. (2013)
  - Further measurements of μp spectroscopy. — Pohl group at MPI Quantenoptik
  - Xext-generation lattice QCD. — Alexandrou et al. (2013), Bhattacharya et al. (2013), Green et al. (2014)
- New physics?
  - New general flavour-conserving nonuniversal interactions. — Barger et al. (2011), Carlson & Rislow (2012)
  - Parity-violating muonic forces. — Batell et al. (2011)
  - MeV-scale force carriers between protons and muons. — Tucker-Smith & Yavin (2011), Izaguirre et al. (2015)